Fusion Engineering and Design 101 (2015) 218–225

Contents lists available at ScienceDirect

Fusion Engineering and Design

journal homepage: www.elsevier.com/locate/fusengdes

# Design, fabrication, and properties of a continuous carbon-fiber reinforced $Sm_2O_3$/polyimide gamma ray/neutron shielding material

Peng Wang [a], Xiaobin Tang [a,b,*], Hao Chai [a], Da Chen [a,b], Yunlong Qiu [c]

[a] Department of Nuclear Science and Engineering, Nanjing University of Aeronautics and Astronautics, Nanjing 210016, China
[b] Jiangsu Key Laboratory of Nuclear Energy Equipment Materials Engineering, Nanjing 210016, China
[c] ZhongXing Energy Equipment Co., Ltd, Haimen, Nantong 226100, China

## HIGHLIGHTS

- $Sm_2O_3$ is used for neutron absorber instead of $B_4C$, and $Sm_2O_3$ has a good photon-shielding effect.
- Carbon-fiber cloth and polyimide were used to enhance shielding materials' mechanical behavior and thermal behavior.
- Both Monte Carlo method and shielding test were used to evaluate shielding performance of the novel shielding material.

## ARTICLE INFO

*Article history:*
Received 8 June 2015
Received in revised form 2 August 2015
Accepted 10 September 2015
Available online 28 September 2015

*Keywords:*
Continuous carbon fiber
Samarium oxide
Polyimide
Gamma ray/neutron shielding material

## ABSTRACT

The design and fabrication of shielding materials with good heat-resistance and mechanical properties is a major problem in the radiation shielding field. In this paper, based on gamma ray and neutron shielding theory, a continuous carbon-fiber reinforced $Sm_2O_3$/polyimide gamma ray/neutron shielding material was fabricated by hot-pressing method. The material's application behavior was subsequently evaluated using neutron shielding, photon shielding, mechanical tensile, and thermogravimetric analysis–differential scanning calorimetry tests. The results show that the tensile strength of the novel shielding material exceeds 200 MPa, which makes it of similar strength to aluminum alloy. The material does not undergo crosslinking and decomposition reactions at 300 °C and it can be used in such environments for long periods of time. The continuous carbon-fiber reinforced $Sm_2O_3$/polyimide material has a good shielding performance with respect to gamma rays and neutrons. The material thus has good prospects for use in fusion reactor system and nuclear waste disposal applications.



## 1. Introduction

As nuclear technology develops, the demand for neutron shielding materials grows and the types of shielding materials required need to be diversified [1,2]. In practice, many situations need the support of high-performance shielding materials, e.g. for the safe disposal of nuclear waste and the safe operation of fusion reactors [3,4]. The domain of application of nuclear technology has been expanding rapidly. As a result, the environments in which shielding materials are used are becoming increasingly harsher [5]. The effectiveness of radiation shielding is subject to strict rules and standards, and there are corresponding requirements for the mechanical properties and heat resistance of the shielding material that must be met [6]. Traditional shielding materials cannot fulfill current development needs. Research and development of neutron shielding material (NSM) with high thermal durability and excellent mechanical properties is the best solution to this problem.

In order to satisfy the needs of different tasks, a series of research investigations on shielding materials were conducted. Pb-B polythene is one of the most widely used shielding materials in the radiation protection field. The Nuclear Power Institute of China manufactured various types of Pb-B polythene composites [7]. However, the maximum temperature for the use of polythene is limited to 100 °C. In addition, the tensile strength of Pb-B polythene composites is relatively low so they cannot satisfy the demands placed on them for most purposes under high temperature and pressure conditions. High density polyethylene has been used to reinforce the mechanical properties and heat resistance of shielding materials, but the increase in performance was limited and so it has not been widely adopted [8,9]. A boron–aluminum composite

* Corresponding author at: Department of Nuclear Science and Engineering, Nanjing University of Aeronautics and Astronautics, 29 Yudao St., Nanjing 210016, China.
*E-mail address:* tangxiaobin@nuaa.edu.cn (X. Tang).

http://dx.doi.org/10.1016/j.fusengdes.2015.09.007
0920-3796/

has been fabricated using powder metallurgy. The manufacturing process is, however, relatively complicated leading to high production costs [10]. In this paper, a novel type of shielding material is designed and fabricated for high-temperature and high-pressure environments based on new materials and methods.

During the 1960–1990s of the last century, polymer technology developed rapidly. Continuous carbon-fiber reinforced polyimide composites have high specific strength, high specific modulus, and excellent high temperature performance and corrosion resistance [11,12]. They are one of several high performance materials that have found wide application. In order to make the design method fit the philosophy of combining structure with function, the use of a continuous carbon-fiber reinforced polyimide resin as the matrix for the shielding material is the best way to improve the mechanical and thermal performance of the material.

## 2. Experimental methods

### 2.1. Design of the shielding material

Neutron shielding theory is different from gamma shielding theory [13]. The effectiveness of a neutron shield mainly depends on neutron-nucleus collisions and neutron absorption. As collision with a light nucleus can decrease the energy of neutrons better, resin is generally chosen as the neutron moderator. After moderation, neutrons are absorbed by nuclei with large neutron absorption cross-sections, e.g. $^{10}B$ and $^{6}Li$. In contrast, gamma radiation shields depend on photon-matter interactions (e.g. the photoelectric, Compton, or electron-pair effects). As the cross-sections of photonic interactions increase with atomic number, heavy metals (e.g. Pb and Bi) are usually employed as gamma ray absorbers. When neutron and gamma ray shielding requirements are considered together, a type of heavy metal with large neutron-absorption cross-section clearly needs to be added into the polymer resin to improve the shielding effect for both neutrons and gamma rays.

Traditional shielding materials use boron carbide as the neutron absorber. However, the atomic number of boron is low and so it does not have a good shielding performance in respect of gamma rays [14]. Some rare earth elements have larger thermal-neutron absorption cross-sections and photon-reaction cross-sections than boron (e.g. Gd, Sm, Eu, and Er). Therefore, a rare earth element may be a good neutron absorber to use instead of boron (see, for example, the absorption cross-section for samarium shown in Fig. 1). Absorption of X-rays and neutrons by rare earth elements has been researched by Beijing University of Chemical Technology [15]. They

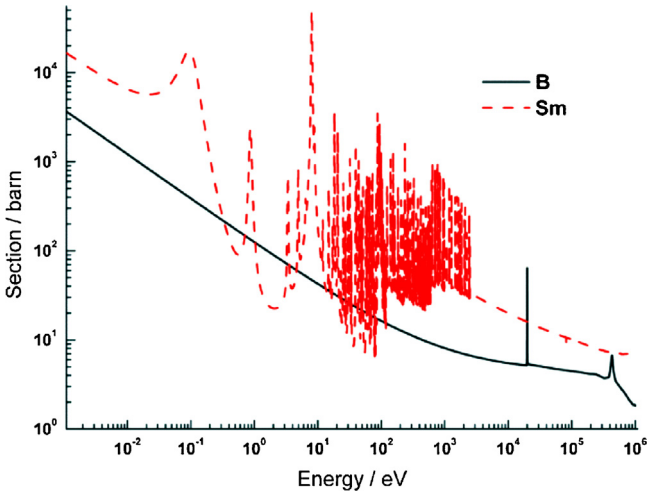


**Fig. 1.** The neutron absorption cross-sections of samarium and boron.

pointed out that although boron reacts with neutrons to produce helium bubbles (which rapidly degrade the mechanical properties of the shielding material), the reaction with rare earth elements has little impact on the material's structure. Thus, using samarium (Sm) as a neutron absorber can ensure that the shielding material has a stable performance for long periods of time.

### 2.2. Raw materials

#### 2.2.1. $Sm_2O_3$ powder (sub-micron)

$Sm_2O_3$ powder would ordinarily sink in the resin and thus be distributed non-uniformly. In order to avoid deposition of $Sm_2O_3$ powder and ensure that the shielding material has good mechanical and shielding properties, sub-micron powder was chosen to manufacture the NSM. The microstructure of the $Sm_2O_3$ powder is shown in Fig. 2.

#### 2.2.2. Thermosetting polyimide resin (model: TY005-1)

Polyimide plastics are a kind of engineering plastic with some special properties. They have excellent thermal-stability, good chemical corrosion resistance, and great mechanical properties. In addition, they can prevent burning without the additional use of a flame retardant. Thermosetting polyimide was thus chosen for the matrix to effectively improve the heat resistance and mechanical properties of the shielding material.

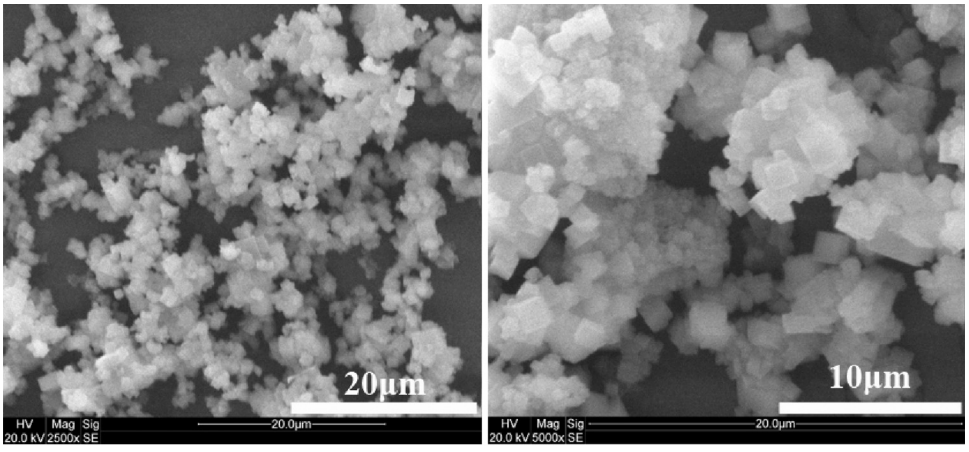


**Fig. 2.** The microstructure of $Sm_2O_3$ powder.

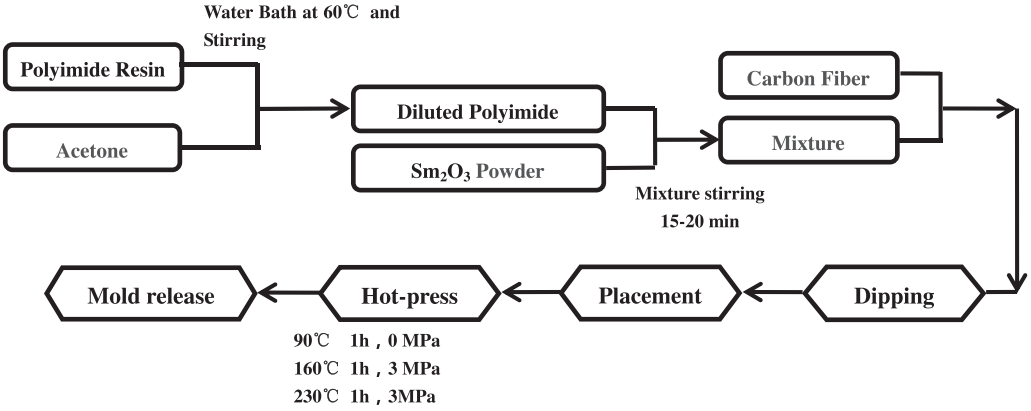


**Fig. 3.** Flow chart showing the method of fabrication of the continuous carbon-fiber reinforced $Sm_2O_3$/polyimide shielding material.

*2.2.3. Acetone*

As the fluidity of polyimide is very poor, a diluent needs to be added for dipping treatment. High purity acetone (≥99.9%) was used as the diluent for polyimide resin, as the polyimide resin is very soluble in this solvent. Provided the performance of the material was not affected, the acetone can be removed by evaporation by heating the material at 90 °C.

*2.2.4. Polyacrylonitrile-based carbon-fiber cloth (0.3 mm thick)*

Continuous carbon fiber was chosen to effectively enhance the mechanical properties of the shielding material. Its use also reduces the material's density as much as possible. Carbon fibers have good resistance to irradiation and heat. Their use, therefore, can allow the NSM to be used in more demanding environments.

*2.3. Preparation of shielding material*

The polyimide resin was too viscous to mix material. According the manufacturer's recommend, the proportion of polyimide resin and acetone was about 4:1. Because the higher volume fraction of the neutron absorbers was better, but the NSM could not been formed if the mass fraction of Samarium oxide powder was higher than 21% in the mixing ratio of polyimide fluid. Hence, the percentage composition was shown in Table 1.

First, the polyimide resin was heated by using water bath until it showed good fluidity. Then, it was poured into a certain quantity of acetone and gently stirred. After cooling to room temperature, $Sm_2O_3$ powder was added to the diluted polyimide resin according to the proportions shown in Table 1. The $Sm_2O_3$ powder was dispersed evenly in the polyimide solution using mechanical stirring. This prefabrication of the NSM was completed.

**Table 1**
The percentage composition of the polyimide fluid.

| Component | Content (wt.%) |
|---|---|
| Polyimide resin | 62.5% |
| Samarium oxide powder | 21% |
| Acetone | 16.5% |

After dipping in the polyimide fluid, the carbon fiber cloth was placed layer upon layer by hand following lay-up technology. A plate vulcanizing machine was used to fabricate the shielding material. First of all, the temperature was set to 90 °C and the pressure 0 MPa for the acetone removal. Then, the pressure was increased to 3 MPa and the temperature raised from 90 °C to 160 °C for pre-curing. Finally, the temperature was set to 230 °C to cure the polyimide (the material preparation process and conditions used are shown in Fig. 3). After demolding, the final continuous carbon-fiber reinforced $Sm_2O_3$/polyimide gamma ray/neutron shielding material was obtained. The microstructure of surface of NSM was given in Fig. 4. The SEM images showed that filler was uniformly distributed in the resin and had no reunion.

*2.4. Shielding experiments*

In order to investigate the shielding ability of the new material, we undertook shielding experiments using an $^{241}$Am-Be neutron source and $^{137}$Cs and $^{60}$Co gamma radiation sources. The neutron and gamma transmissivity were used to evaluate the radiation shielding performance of the novel material.

$^3$He has a large neutron-absorption cross-section and so a $^3$He proportional counter was used to detect neutrons. The neutron

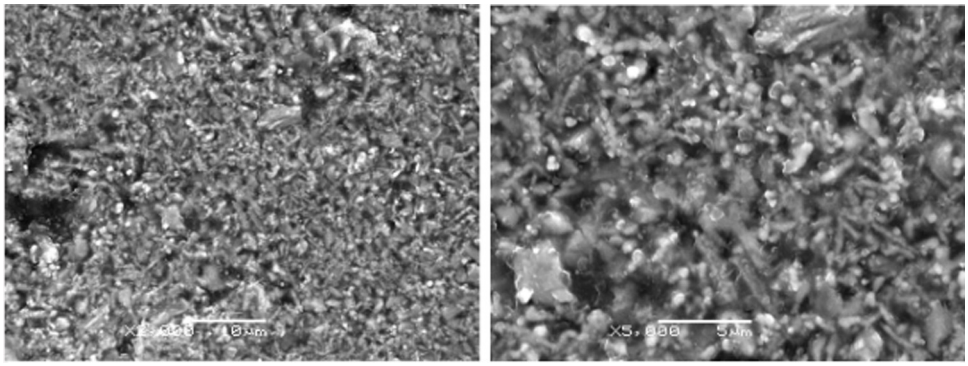

**Fig. 4.** The microstructure of surface of NSM.

**Fig. 5.** The MCNP geometric model and a photo of the neutron detection equipment.

yield from the Am-Be neutron source was 50 μCi. The $^{3}$He proportional counter was surrounded with a 1 cm thick layer of pure boron carbide apart from the direction facing the neutron source. A 5.5 cm × 7.5 cm sheet of shielding material was placed between the Am-Be neutron source and $^{3}$He proportional counter (as shown in Fig. 4). The thickness of the NSM was gradually increased and the neutron count recorded at each thickness using a detection time of 300 s.

A scintillator detector (3 × 3 NaI (Tl)) and two different types of gamma source ($^{137}$Cs with a characteristic gamma energy of 662 keV, and $^{60}$Co with gamma energies of 1170 and 1330 keV) were used to test the gamma shielding performance. The activities of the two different types of radiation source were 2 μCi, the distance between the radiation source and the detector was 36 cm, and the detection time was 600 s. The full-energy peak count was used to evaluate the gamma ray shielding performance.

In addition, as calculations can reveal more detail than experimental data alone, a Monte Carlo method was used to calculate the shielding performance of the novel gamma ray/neutron shielding material. The calculation software was MCNP/4C, and the library of cross-section was ENDF/B-VI. A geometric model was built based on the shape and size of the detection equipment, as shown in Figs. 5 and 6.

### 2.5. Mechanical experiments

A tensile testing machine was used to test the tensile properties of the NSM. Composites with five different numbers of carbon-fiber cloth layers (1, 2, 4, 6, and 8 layers, respectively) were tested and the number of each sample was five. The maximum tension of electron universal testing machines was 100 kN, which was much larger than tensile strength of NSM, the speed of the loading was 2 mm/min during the tests. The NSMs were cut into dumbbell-shaped specimens (see Fig. 7), where $L0$ = 50 mm, $L1$ = 55 mm, $L2$ = 55 mm, $L3$ = 115 mm, $B0$ = 10 mm, and $B1$ = 20 mm.

### 2.6. TAG–DSC thermostability experiments

Thermal stability is very important for polymers and is an important property to evaluate for applications. Differential scanning calorimetry was used in this work to investigate the thermal stability of the NSM. The experimental parameters were set so that the heating rate was 10 °C/min, the sample quantity was 10 mg, the

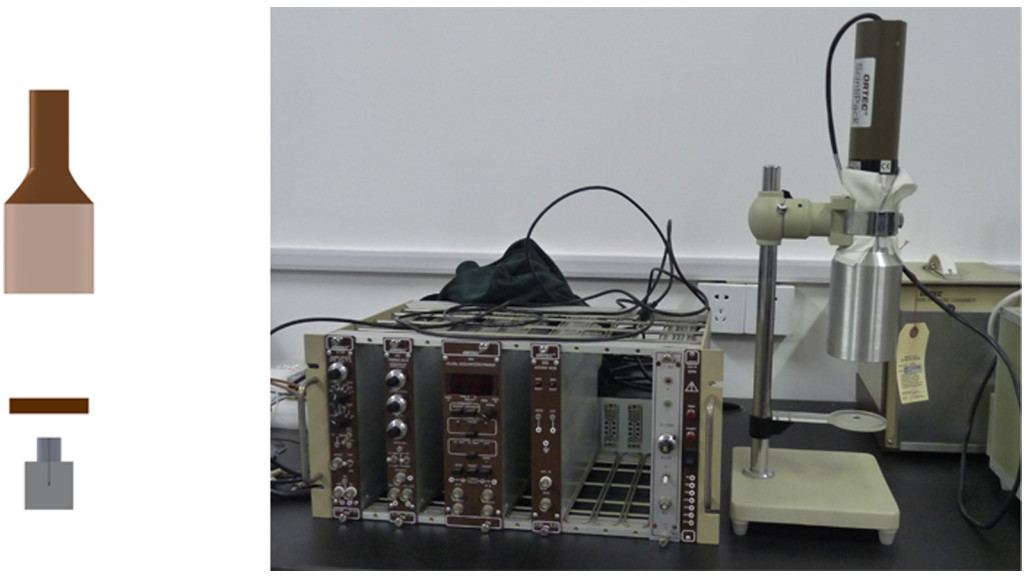

**Fig. 6.** The MCNP geometric model and a photo of the gamma ray detection equipment.

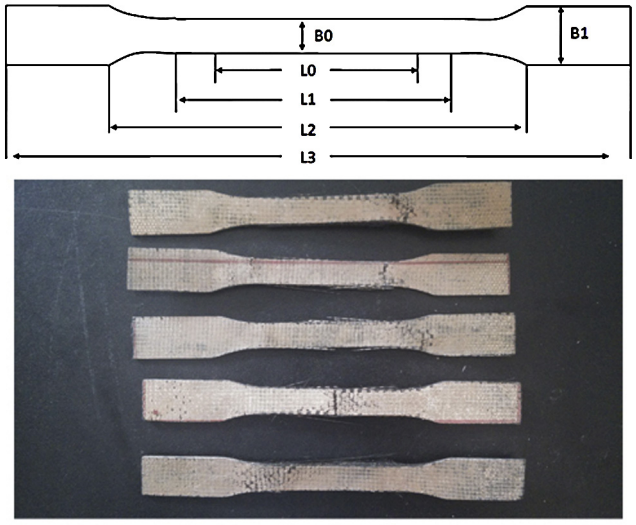


**Fig. 7.** The geometric size of sample and a photo of the dumbbell-shaped specimens.

atmosphere was air, and the temperature range scanned was from 30 to 450 °C.

## 3. Experimental results and discussion

According to theory, neutron transmissivity decreases with material thickness (see Fig. 8). The change in neutron transmissivity with thickness is described more quantitatively by

$$\eta = I_i/I_0 = Be^{-\Sigma d_i} + a, \quad (1)$$

where $\eta$ is the transmittance of gamma, $I_i$, $I_0$ are the count rate of before and after shielding, $B$ is cumulative factor, $d_i$ is the thickness of the shielding material, $a$ is the background count, and $\Sigma$ is the macroscopic cross-section (representing the neutron shielding ability for a specific energy range).

In Fig. 8(b), the neutrons were divided into four groups according to their energy. The transmissivity of neutrons of all energies decreased with the material thickness but the low-energy neutrons were absorbed most efficiently. This is because the neutron absorption cross-section decreases with increasing neutron energy. Table 2 lists the macroscopic cross-sections of the shielding material for neutrons of different energy (from calculated data).

As the average energy of the neutrons emitted by the Am-Be neutron source was 4.5 MeV, no matter where the $^3$He proportional counter was moved to in the laboratory, some neutrons were still able to enter the detector after being scattered. In the beginning, the number of background neutrons was detected using a $^3$He proportional counter, and then we began testing the shielding samples. As shown in Fig. 8(a), when 3 cm of shielding material was used, the neutron irradiation level had fallen to the environmental level.

**Table 2**
Macroscopic cross-sections for different energies (based on simulated data).

| Neutron energy (keV) | Macroscopic cross-section ($cm^{-1}$) |
|---|---|
| <0.01 | 1.86 |
| 0.01–1 | 1.32 |
| 1–1000 | 0.21 |
| >1000 | 0.12 |

Comparing Fig. 8(a) and (b), it can be seen that the experimentally measured values of neutron transmissivity are different to the values calculated using the Monte Carlo codes (MCNP/4C). However, the neutron transmittances whose energy less than 10 eV were similar with the experimental results. This is because $^3$He has larger thermal neutron absorption cross-sections, that is, the $^3$He proportional counter only reflects the shielding performance for low-energy neutrons but neutrons of all energy are included in the calculations.

The macroscopic cross-sections for the experimental and simulated curves are 0.88 $cm^{-1}$ and 0.15 $cm^{-1}$, respectively. This demonstrates that the $^3$He proportional counter mainly records the low-energy neutrons. Generally, the $^{241}$Am-Be neutron transmittance of 3 cm of the Pb-B polythene composites is about 60% [16], that is roughly the same with the neutron shielding ability of NSM.

Overall, the continuous carbon-fiber reinforced $Sm_2O_3$/polyimide neutron/gamma ray shielding material has good thermal neutron shielding performance. It is also capable of absorbing some of the higher-energy neutrons. In practical engineering applications, the designers can obtain radiation fields according the structure of the fusion reactor [17], and then decided the thickness of NSM to ensure the health of the operator.

Fig. 9(a) shows the experimental shielding efficiency of the new shielding material with respect to gamma photons. Clearly, the transmissivity of the photons declines as the shielding thickness increases. The absorptive capacity of the NSM is greater for low-energy gamma radiation compared to high-energy gamma radiation. When the thickness of the NSM is 5 cm, 57.6%, 65.6%, and 67.8% of the gamma radiation at 662, 1170, and 1330 keV is transmitted, respectively.

The experimental and calculated values of gamma transmittance were accordant basically and also have the same change tendency as shown in Fig. 9(b). However, the calculated values were slightly different to the experimental data. The calculation model

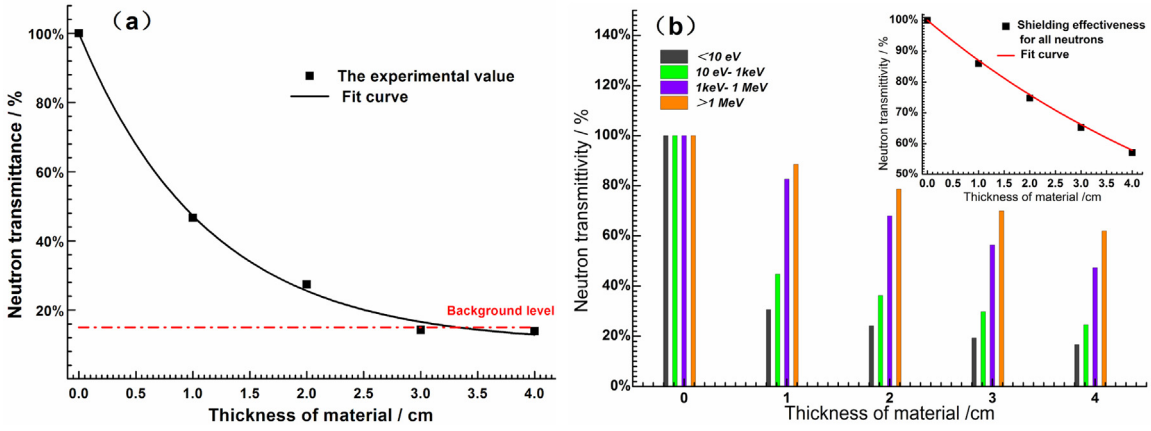


**Fig. 8.** The neutron shielding properties of continuous carbon-fiber reinforced $Sm_2O_3$/polyimide shielding material: (a) experimental values, and (b) calculated values.

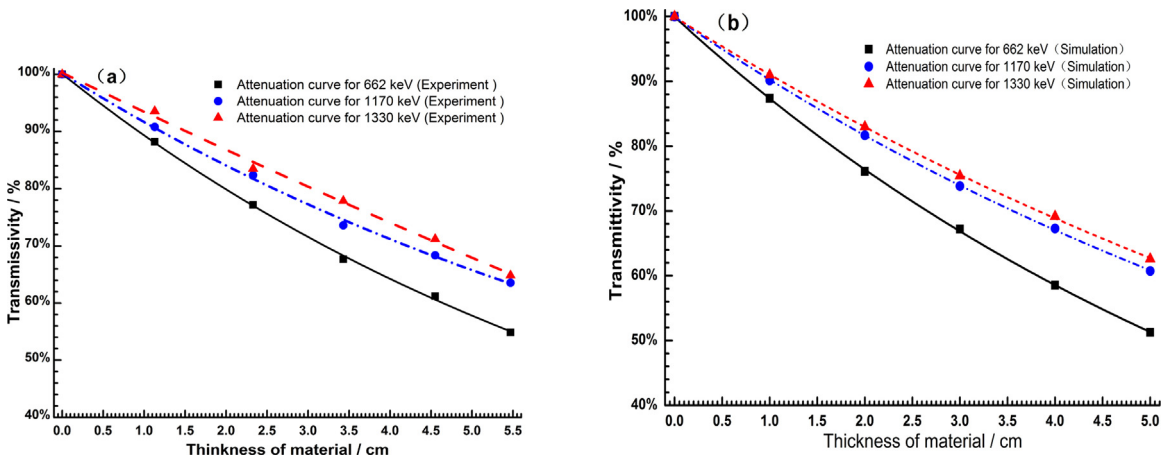


**Fig. 9.** The gamma ray shielding performance of the continuous carbon-fiber reinforced $Sm_2O_3$/polyimide shielding material: (a) experimental values, and (b) calculated values.

established was slightly different to the prepared composite material. For example, the elements of the material were uniform in the calculation model, but the prepared composite is not completely uniform (that is, the continuous carbon fiber contains most of the elemental carbon and the $Sm_2O_3$ powder contains all of the samarium). This difference is the main source of the variation. As shown by the results from the calculations and experiments, the NSM has a good shielding effect for medium-energy and low-energy gamma rays.

The tensile strength of the material is affected by two factors: the presence of defects and stress concentration. The number of defects increased gradually with the number of carbon-fiber cloth lays. In Fig. 10(a), the tensile strength of the NSM can be seen to increase with the number of carbon-fiber layers used.

When a single carbon-fiber layer is used, stress conduction does not occur in the material, so the tensile performance of the material is very poor. However, doubling the number of carbon-fiber layers to two greatly improves the tensile strength. The number of carbon-fiber layers continues to increased, the tensile strength of the shielding material increases more slowly. This is because the conduction ability of the resin is limited and the defects increases. The carbon-fibers were connected together by resin as shown in Fig. 11, and the resin could transfer stress effectively. However, some holes could be found in NSM's fracture surface. The reason is that many defects in the NSM leaded to some carbon-fibers were pulled out. The tensile strength of the NSM is greater than 200 MPa (roughly equal to the tensile strength of traditional aluminum alloy) and so it does meet the demand for high strength.

The tensile modulus of the NSM is shown in Fig. 10(b). Clearly, the modulus gradually increases with the number of carbon-fiber layers. As a result of stress conduction between carbon fibers within the resin, stress concentration is greatly reduced. However, as the number of carbon-fiber layers increases, the change in stress transmission range is limited, and the tensile modulus tends to stabilize. The elastic modulus of the carbon fibers is greater than that of the resin, and the stiffness of the carbon fibers enhances the stiffness of the composite material greatly. The shielding material can thus maintain its shape better and continue to function when used in demanding applications.

There are two kinds of reaction that polymers may undergo at high temperature. One of these is crosslinking, and the other is decomposition. Crosslinking is where the polymer chains link to one another to form a 3D net structure; decomposition is where the polymer chains undergo molecular scission. The initial temperatures corresponding to crosslinking and decomposition reactions were observed by recording TGA and DSC curves, and the maximum service temperature of the NSM was determined.

As shown in Fig. 12, the quality of the NSM initially decreased slowly with temperature because volatilization of the acetone used was not fully complete. However, the quality of the NSM subsequently declined rapidly at 330 °C due to decomposition of the polyimide matrix. Heat flow declined with an increase in the temperature in the DSC curve, and there were no obvious endothermic

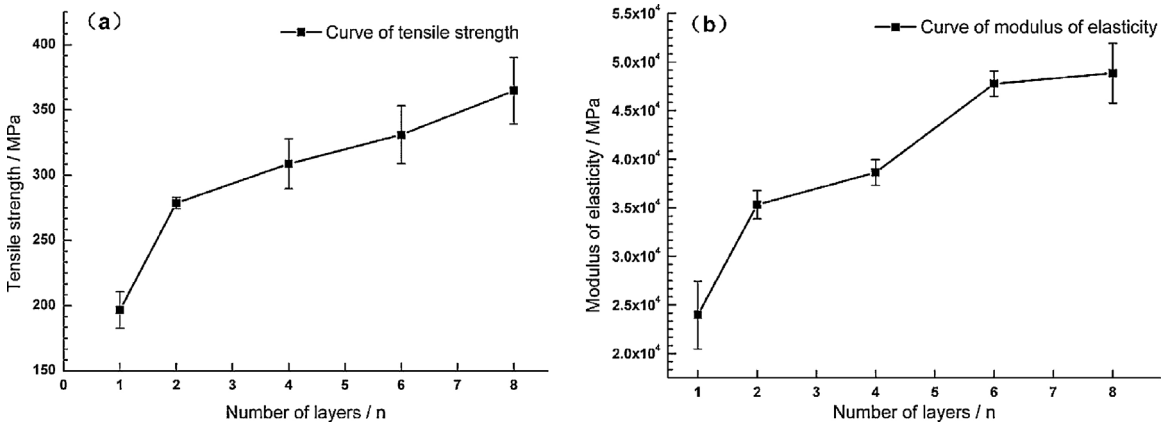


**Fig. 10.** Curves showing the mechanical performance of the continuous carbon-fiber reinforced $Sm_2O_3$/polyimide shielding material: (a) the tensile strength, and (b) the modulus of elasticity.

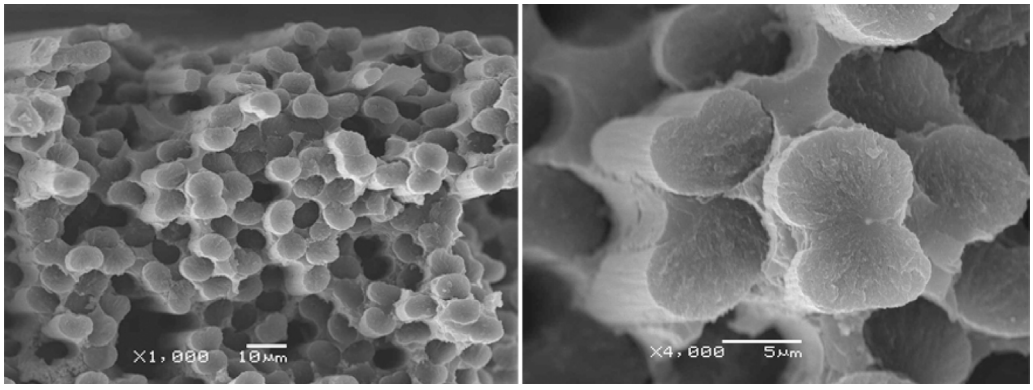


**Fig. 11.** The microstructure of NSM's fracture surface.

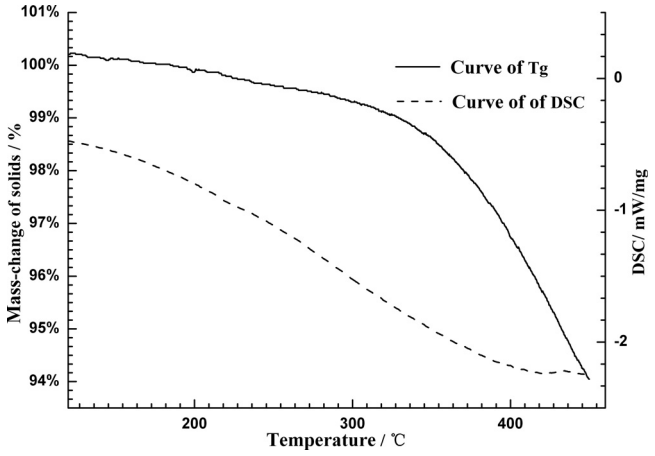


**Fig. 12.** Results of the TGA–DSC tests on the $Sm_2O_3$/polyimide shielding material.

or exothermic peaks. This suggests that the polyimide resin in the new shielding material had been completely cured in the process of fabrication and there were no glass transitions or crosslinking reactions up to 450 °C. Overall, the new material's heat-resistant temperature is considered to be 300 °C, and so the material is able to work stably up to 300 °C.

## 4. Conclusions

In conclusion, in accordance with the principles underlying gamma radiation and neutron shielding, the rare earth element and heavy metal samarium was adopted during the design of a NSM which was subsequently fabricated using a plate vulcanizing machine. A variety of tests (gamma shielding experiments, neutron shielding experiments, tensile tests, and thermal stability experiments) were used to evaluate the application performance of the continuous carbon-fiber reinforced $Sm_2O_3$/polyimide material. The experimental results revealed that when the thickness of the shielding material was 3 cm, the number of neutrons recorded at the detector was equal to the environmental level. The continuous carbon-fiber reinforced $Sm_2O_3$/polyimide gamma/neutron shielding material has a good shielding effect for low-energy gamma photons. As expected, gamma ray transmissivity declined exponentially with the thickness of the shielding material. In addition, as polyimide resin has excellent heat resistance and carbon fiber has great specific strength, these components greatly improved the mechanical properties and heat-resisting performance of the NSM. The traditional shielding material such as the Pb-B polythene composites and high density polyethylene composites, their tensile strength are 10–25 MPa, the using temperature are about 100 °C. However, the NSM's tensile strength is above 200 MPa, that is about ten times higher than Pb-B polythene composites and high density polyethylene composites. The maximum service temperature is 300 °C, the higher using temperature can largely expand shielding material application scope. Therefore, the experimental results indicate the NSM is a good candidate for radiation shielding of fusion reactor.

## Acknowledgements

This work was supported by National Defence Basic Scientific Research Project [Grant No. B2520133007]; the Specialized Research Fund for the Doctoral Program of Higher Education of China (SRFDP) [Grant No. 20123218120028]; the Funding of Jiangsu Innovation Program for Graduate Education and the Fundamental Research Funds for the Central Universities [Grant No. KYLX_0266]; and the cooperative innovation fund project of Jiangsu Province [Grant No. BY2014003-04].

## References

[1] T. Korkut, O. Gencel, E. Kam, W. Brostow, X-ray, gamma, and neutron radiation tests on epoxy-ferrochromium slag composites by experiments and Monte Carlo simulations, Int. J. Polym. Anal. Charact. 18 (2013) 224–231.
[2] M. El-Sarraf, A. El-Sayed Abdo, Influence of magnetite, ilmenite and boron carbide on radiation attenuation of polyester composites, Radiat. Phys. Chem. 88 (2013) 21–26.
[3] M. Zucchetti, A. Ciampichetti, Safety and radioactive waste management aspects of the ignitor fusion experiment, Fusion Sci. Technol. 56 (2009) 814–818.
[4] M. Andreev, V. Afanasiev, A. Belevitin, A. Karaulov, V. Romodanov, V. Sakharov, G. Tikhomirov, A. Vasiliev, Y.Z. Kandiev, V. Lyutov, Set of benchmark experiments on slit shielding compositions of thermonuclear reactors, Fusion Eng. Des. 55 (2001) 373–385.
[5] Y. Huang, W. Zhang, L. Liang, J. Xu, Z. Chen, A "Sandwich" type of neutron shielding composite filled with boron carbide reinforced by carbon fiber, Chem. Eng. J. 220 (2013) 143–150.
[6] Y.H. Duan, Y. Sun, M.J. Peng, Z.Z. Guo, Mechanical and shielding properties of an As-cast new Pb-B shielding composite materials, Adv. Mater. Res. 150 (2011) 56–63.
[7] L. Jixin, C. Jianting, High effective shielding material lead-baron polyethylene, Nucl. Power Eng. 4 (1994).
[8] Q.-r. Zhang, C.-l. Tang, X.-y. Chen, H.-d Ma, Y.-s. Han, Study on preparation of composite plates with neutron shielding function, Chem. Eng. 9 (2009) 028.
[9] J.W. Shin, J.-W. Lee, S. Yu, B.K. Baek, J.P. Hong, Y. Seo, W.N. Kim, S.M. Hong, C.M. Koo, Polyethylene/boron-containing composites for radiation shielding, Thermochim. Acta 585 (2014) 5–9.
[10] P. Zhang, Y. Li, W. Wang, Z. Gao, B. Wang, The design, fabrication and properties of $B_4C$/Al neutron absorbers, J. Nucl. Mater. 437 (2013) 350–358.

[11] J. Li, X. Cheng, Effect of rare earth solution on mechanical and tribological properties of carbon fiber reinforced thermoplastic polyimide composite, Tribol. Lett. 25 (2007) 207–214.
[12] S. Chand, Review carbon fibers for composites, J. Mater. Sci. 35 (2000) 1303–1313.
[13] J.E. Martin, Physics for Radiation Protection, John Wiley & Sons, 2013.
[14] X. Cao, X. Xue, T. Jiang, Z. Li, Y. Ding, Y. Li, H. Yang, Mechanical properties of UHMWPE/$Sm_2O_3$composite shielding material, J. Rare Earths 28 (2010) 482–484.
[15] L. Li, S. Zhaohui, W. Youping, Radiation shielding and magnetic properties of rare earth/polymer composites, China Synth. Rubber Ind. 3 (2001) 027.
[16] L. Yuanyuan, Z. Changgui, Y.J. Dai Shengping, Shielding performance of boron polyethylene and lead–boron polyethylene by test and simulation, Radiat. Prot. 1 (2013) 006.
[17] C. Yixue, W. Yican, H. Qunying, Monte Carlo Analysis of Environmental Dose Rate of HT-7U Fusion Device, 2005.